

Journal Pre-proof

Role of fiber inclusion in adobe masonry construction

Innocent Kafodya, F. Okonta, Panos Kloukinas



PII: S2352-7102(19)30248-7

DOI: <https://doi.org/10.1016/j.jobe.2019.100904>

Reference: JOBE 100904

To appear in: *Journal of Building Engineering*

Received Date: 15 February 2019

Revised Date: 29 July 2019

Accepted Date: 30 July 2019

Please cite this article as: I. Kafodya, F. Okonta, P. Kloukinas, Role of fiber inclusion in adobe masonry construction, *Journal of Building Engineering* (2019), doi: <https://doi.org/10.1016/j.jobe.2019.100904>.

This is a PDF file of an article that has undergone enhancements after acceptance, such as the addition of a cover page and metadata, and formatting for readability, but it is not yet the definitive version of record. This version will undergo additional copyediting, typesetting and review before it is published in its final form, but we are providing this version to give early visibility of the article. Please note that, during the production process, errors may be discovered which could affect the content, and all legal disclaimers that apply to the journal pertain.

© 2019 Published by Elsevier Ltd.

Role of fiber inclusion in adobe masonry construction

Innocent Kafodya^{1*}, F Okonta¹, Panos Kloukinas²

¹ Civil Engineering Science Department, University of Johannesburg, South Africa

P.O Box 524, Auckland Park, 2006, South Africa

² Faculty of Engineering and Science, University of Greenwich, United Kingdom

Abstract

Adobe masonry construction constitutes a notable portion of the buildings in both urban and rural areas in less developed countries. Seismic performance of adobe buildings is poor, and low-cost retrofitting measures are required to enhance the resilience of such buildings during an earthquake. In this study, mechanical properties of fiber reinforced and unreinforced adobe masonry were investigated. Sisal fibers with length of 25mm were used as reinforcing elements for mortar and adobe bricks at a fiber content of 0.75%. A series of laboratory tests were performed on masonry triplets, couplets and prisms to determine shear strength, tensile resistance and compressive strength, respectively. Uniaxial compression and diagonal compression shear tests were performed on wallets and wall panels, respectively to determine compressive strength and shear strength of the adobe masonry. Finite element linear elastic analysis was conducted using ANSYS Finite-Element code to evaluate the stress state of loaded wall panels. The structural design of adobe masonry walls was carried out according to BS5628 and Eurocode 6 standards, by utilising material properties acquired from the experiments. The results showed that fiber inclusion in the mortar caused an increase in tensile strength of 31%, friction coefficient of 22%, and prism compressive strength of 25% compared with unreinforced mortar. The reinforced wallets exhibited a twofold increase in compressive strength while reinforced

24 wall panels indicated threefold increase in shear strength. The stress state in the reinforced and
25 unreinforced wall panels was not a pure shear state and was better described by RILEM
26 recommendations. The allowable vertical load resistance was found to be 40kN/m and 100kN/m
27 for unreinforced and reinforced walls, respectively. The allowable lateral shear resistance was
28 found to be 25kN/m and 80kN/m for unreinforced and reinforced walls, respectively. Reinforced
29 masonry elements exhibited considerable ductility and unreinforced masonry elements showed
30 brittle behaviour.

31

32 **Keywords:** adobe bricks, masonry, fiber reinforcement, mortar.

33 *Corresponding author, E-mail: ikafodya@poly.ac.mw; Tel: +27115592318

1. Introduction

34 Adobe is the oldest and widely used material for construction of dwelling houses. It is estimated
35 that one third of the world's population and 50% of the population in the developing countries
36 still live in the earthen buildings[1]. Earthen construction offers manifold benefits including cost
37 effectiveness, lower embodied energy levels, high thermal mass and reduced use of non-
38 renewable materials[2-4]. The interest in earthen construction in the developed countries has
39 been driven by the demands for more sustainable form of built environment. In this regard,
40 earthen materials have been the attractive alternative to conventional high energy demand
41 construction materials[2]. Moreover, it is expected that the earthen structures in developing
42 countries will continue to exist not only due to their economic benefits, but also because of
43 cultural tradition and identity attached to them[5]. The application of adobe materials faces
44 several constraints due to their brittle behaviour, low tensile strength and deterioration when
45 exposed to moisture. However, the properties of adobe can be improved by mechanical
46 compaction, chemical stabilisation with cement, lime and bitumen, and fiber inclusions such as
47 straw [3, 6]. Chemical stabilisation can significantly improve strength and water resistance of
48 adobe. Typically, chemical binders are added at the contents between 4 and 10% of the soil dry
49 weight [7, 8]. On the other hand, the use of these additives significantly increases both material
50 cost and environmental impact. Alternatively, natural fiber inclusions have been used in earthen
51 construction to increase ductility, tensile strength, postcrack strength, erosion resistance,
52 dimensional stability and reduce shrinkage cracks of the material[4].

53 The previous studies [9, 10] focused on the solution to improve mechanical properties of adobe
54 bricks with natural fibers and chemical additives. The existing literature [11, 12] reports much on
55 the seismic behaviour of adobe structures and the development of seismic strengthening

56 solutions. In practice, the performance of adobe masonry in tension and shear is governed by the
57 properties of the mortar [13]. Therefore, it is recommended that the strength of the mortar should
58 be less than the strength of masonry units. On the contrary, some proposals have promoted the
59 use of mortars with strengths similar to or greater than the bricks. To date, there is little published
60 scientific data to support these recommendations or published design values for flexural bond
61 strength of adobe brick masonry [2]. The study on cement stabilised mortar shows that tensile
62 bond strength of cement mortar and adobe bricks/blocks varies between 0.007 and 0.032MPa
63 and flexural bond strength between 0.004 and 0.014MPa[2]. The bonding properties of
64 unstabilised mortar with adobe bricks/blocks have not been extensively reported. In particular,
65 synergic strength contributions of fiber reinforced mortar and adobe bricks/blocks to the global
66 performance of the adobe masonry structures have not been reported in the literature. The adobe
67 masonry structures are poorly constructed in the developing countries due to lack of design and
68 construction guidelines. This has rendered the structures vulnerable to natural hazards such as
69 earthquakes[14].

70 This study aimed at providing information on the mechanical properties of fiber reinforced adobe
71 masonry construction for the design of resilient and sustainable low-cost infrastructure. Sisal
72 fibers were used to reinforce mud mortar and adobe bricks. The study focused on the
73 investigation into the effect of fiber inclusion in mud mortar and adobe bricks on the strength
74 improvement of the adobe masonry structure. This was achieved by performing series of
75 masonry element tests such as prism, triplet and couplet to determine compressive, shear and
76 tensile strengths, respectively. The uniaxial compression test on wallets and diagonal
77 compression (shear) test on masonry wall panels were performed to determine compressive
78 strength and shear resistance of the adobe masonry structures. A finite element analysis of the

79 wall panels was conducted to evaluate the stress state of the loaded reinforced and unreinforced
80 masonry wall panels. The results of numerical analysis were compared with ASTM and RILEM
81 interpretations using Mohr circles. Finally, design of the masonry walls was carried out
82 according to BS5628 and Eurocode 6 standards in order to estimate load carrying capacity of the
83 full scale adobe wall.

84 **2. Materials and experimental programme**

2.1. Materials

85 The soil used to manufacture adobe bricks was locally collected and air dried for 48h. The soil
86 was manually sieved to remove any organic particles. Wet sieving for the soil was eventually
87 carried out in accordance with ASTM D1140-17 and the grading curve of the soil is shown in
88 Fig. 1. The soil is classified as CL in accordance with Unified Soil Classification System
89 (USCS). The average diameter of particles at D_{50} is less than 0.075mm. The soil properties are
90 summarised in Table 1.

91 Commercially available fiber used herein was sisal that was supplied by a South African
92 company in the form of ropes. The fibers were cut into specified length of 25mm. Single fiber
93 tensile tests were conducted to determine fiber mechanical properties and the summary of the
94 results is shown in Table 2.

2.2. Preparations and characterisation of masonry constituents

96 The constituents of masonry elements comprised of reinforced and unreinforced mud mortar and
97 adobe bricks. In the manufacture of adobe bricks, dry soil was weighed in the gauge box of
98 dimensions 300x300x300mm. The prescribed fiber content (0.75%) for the adobe composite mix
99 was subsequently determined by the percentage of dry mass of soil, given by Eq. 1.

$$\rho = \frac{m_f}{m_s} \quad (1)$$

101 where m_f is the total mass of fibers and m_s is the mass of the soil in the gauge box.

102 The soil was mixed with water at the moisture content of +2% plastic limit and fibers were
103 gradually added to wet soil until a homogeneous composite paste was formed. The soil paste was
104 cast into a mould of dimensions 215x102x65mm according to BIS recommendation and was
105 immediately demoulded to produce adobe brick. The adobe bricks produced (see Fig. 2) were
106 covered with grass and sun dried for 28days. After drying, the average dimensions of the adobe
107 bricks were reduced to 200x100x60mm due to shrinkage of the material. The local methods for
108 moulding and curing of adobe bricks were adopted to emulate common practice in rural areas of
109 the Eastern and Southern regions of Africa. The unreinforced adobe bricks were also
110 manufactured by following the same moulding and curing procedures.

111 The fiber reinforced and unreinforced mud mortar were also prepared and cast into cubes of
112 50x50x50mm. The mud mortar specimens were prepared in the same manner as the bricks. A
113 total of 6 specimens per mortar type were prepared and cured for 28days under uncontrolled
114 laboratory temperature. This number of specimens was selected in order to obtain good statistical
115 data of the test results. The compression tests were performed on mortar and adobe bricks in
116 order to characterise their strength properties. The irregularities of manufactured adobe brick
117 specimens were smoothed by abrasion before testing to avoid pre-mature failure. The typical
118 strength properties for mortar and adobe bricks used for masonry specimens are shown in Fig. 3.

119 *2.3. Specimen preparation for adobe masonry testing*

120 Masonry elements, namely prisms, triplets and couplets were prepared using the manufactured
121 adobe bricks and aforementioned mortar types (reinforced and unreinforced). Different

122 reinforcement patterns for the prism specimens were adopted. The specimens' reinforcement
123 patterns were as follows; (a) reinforced brick and mortar (coded as RBRM), (b) unreinforced
124 brick and reinforced mortar (coded as UBRM), (c) reinforced brick and unreinforced mortar
125 (coded as RBUM) and, (d) unreinforced mortar and bricks (coded as UBUM). The variations in
126 the reinforcement patterns of masonry prism components aimed at determining the optimum
127 fiber reinforcement design for masonry construction. The masonry elements were cured for
128 28days under uncontrolled laboratory temperature.

129 Two sets of wallets of average dimensions of 500x480x200mm were prepared, one with both
130 reinforced mortar and bricks that was labeled as (RMRB) and the other with both unreinforced
131 mortar and bricks that was labeled as (UMUB). The wall panels of average dimensions of
132 1080x1100x100mm were prepared. Since failure of the wall panels in diagonal shear is
133 governed by strength of the mortar [15], the panel reinforcement was applied to mortar only. The
134 unreinforced adobe bricks were used to prepare panel specimens according to RILEM[16]
135 recommendation. The panel specimens were labeled as UBUM and UBRM to stand for the
136 unreinforced and reinforced panels, respectively. The local procedure used in the Eastern and
137 Southern Africa for masonry construction was adopted. A total of 3 specimens per type were
138 prepared for both wallet and panel testing.

139 *2.4. Experimental programme*

140
141 The compression test of adobe bricks was carried out using Coopers TC4131 compression
142 machine at the stress rate of 0.5kPa/s according to[17]. Compression test on mortar specimens
143 was performed using Quasar 10 universal tensile machine at a loading rate of 0.5mm/min
144 according to [18]. The average compressive strength value of 6 tested specimens was determined
145 and taken as representative strength of materials for both bricks and mortar.

146 The tension capacity of mortar was determined by a series of couplets tests using fabricated test
147 rig. The test set-up for couplets is shown in Fig. 4. The tension bond resistance of the mortar was
148 computed as the sum of measured load and the selfweight of the bottom brick. The tensile bond
149 strength was determined by dividing total load with mortar-brick contact area. The average
150 strength value of 5 specimens of each mortar type was determined and taken as representative
151 strength of the material.

152 The prism and triplet tests were conducted according to [19] and [20], respectively. The triplet
153 was realised with three bricks and two mortar joints. The wooden blocks of 50mm width were
154 placed under the lateral bricks and the load was applied on top of the central brick. Three lateral
155 confinement stresses of 0.025kPa, 0.05kPa and 0.1kPa were applied to determine the coefficient
156 of friction and failure criteria of each mortar type. The test set-up for triplets is shown in Fig. 5.
157 The shear strength of the triplet was computed using Eq. 2.

$$158 \quad \tau_t = \frac{P_{ult}}{2A_g} \quad (2)$$

159 where P_{ult} is the ultimate load and A_g is the area parallel to the mortar joint.

160 Diagonal compression test was performed on wall panels to determine shear strength in
161 accordance with [21]. The diagonal compression test set-up is shown in Fig. 6. The metallic
162 shoes of length 1/10 of the panel length were anchored to the lower and upper corners of the
163 panel by the tension cables. The load cells and the metallic shoes were fixed to the cables by
164 steel pins. The metallic shoes were used in order to distribute the load on a larger surface area to
165 avoid concentration of compression stresses and, consequently, local failures at the corners. The
166 diagonal compression load was applied on the lower corner of the wall by a hydraulic jack until
167 failure of the panel occurred. Shear strength of the panel was computed using Eq. 3 according to

168 ASTM.

$$169 \quad \tau_p = 0.707 \frac{P_t}{A_p} \quad (3)$$

170 where P_t is the ultimate failure load and A_p is the net area of the panel.

171 Displacements and strains of the prism, triplet and wall panel specimens were measured using an
172 Imetrum Video Gauge system, during testing, along with the applied loads measured by
173 calibrated load cells. Numerical simulation of the panels was performed by Finite-Element code
174 ANSYS 14 in ANSYS Parametric Design Language (APDL). The objective was to evaluate the
175 stress state of the wall panels by linear elastic analysis. Both bricks and mortar were modelled
176 using four node triangular standard elements called Plane 183. These elements have two degrees
177 of freedom per node, four Gauss integration points and Lagrangian polynomials as shape
178 functions. The model of the masonry wall was built as a regular inclusion of bricks into a matrix
179 of mortar. The mortar was perfectly bonded to bricks. The geometrical configuration and the
180 boundary conditions were identical to the real experimental setup used in the laboratory testing.
181 The maximum shear loads obtained from the experimental results were applied to the finite
182 element model. The elastic material properties such as Young's modulus and Poisson's ratio that
183 were employed in the finite element analysis are summarised in Table 3.

3. Results and discussions

184 *3.1. Couplet test*

185 The results of tensile capacity of both reinforced mortar (RM) and unreinforced mortar (URM)
186 from couplet tests are shown in Table 4a and 4b. The tensile capacity values of reinforced
187 specimens range between 32N and 41N while values of unreinforced specimens range between

188 20N and 37N. The average tensile resistance values for both unreinforced and reinforced mortar
189 types are 28.2N and 37N, respectively. Fiber inclusion causes an increase in tensile capacity of
190 about 31% compared with unreinforced specimens. The coefficient of variation (COV) of
191 unreinforced specimens is 26% while that for reinforced specimens is 11%. This implies that test
192 results of unreinforced specimens exhibited higher dispersion than for reinforced ones. The fiber
193 inclusion in mud mortar reduces shrinkage of the soil and also minimises size of shrinkage
194 cracks [8]. The lower resistance exhibited by unreinforced mortar was due to the shrinkage of the
195 mortar that undermined bonding at mortar-brick interface. The presence of shrinkage cracks
196 caused pre-mature failure of the unreinforced mortar. The variations in the bonding properties of
197 the unreinforced mortar resulted in the high dispersion of test results. On the other hand, the low
198 shrinkage and significant tensile resistance of fibers were responsible for good bonding at the
199 mortar-brick interface and high tensile resistance of the fiber reinforced mortar.

200 3.2. Triplet test

201 The test results of shear strength of reinforced and unreinforced mortar types are shown in Tables
202 5a and 5b, respectively. For the reinforced specimens, shear strength with lateral confinement
203 stresses between 0.025kPa and 0.1kPa ranges between 0.035kPa and 0.105kPa. On the other
204 hand, the shear strength of unreinforced specimens with lateral confinement stresses between
205 0.025kPa and 0.1kPa ranges between 0.028kPa and 0.085kPa. The shear strength values of adobe
206 masonry between 0.014kPa and 0.05kPa are reported in the literature [22]. The marginal
207 difference between the literature and the test results is attributed to the type of soil and the lateral
208 confinement stresses imposed on the specimens in the present study. The corresponding Mohr-
209 Coulomb failure criteria for both mortar types are shown in Fig. 7. It is shown that an increase in
210 lateral confinement stress causes an increase in shear strength. It is worth noting that the angles

211 of friction for reinforced and unreinforced specimens are 39° and 32° , respectively. In
212 comparison, fiber reinforced specimens indicate an average increase in shear strength of about
213 22% relative to unreinforced specimens. The cohesion of about 0.037MPa and 0.025MPa for
214 reinforced and unreinforced mortar respectively, are indicated. The angles of friction between
215 29° and 34° , and cohesion values between 0.037MPa and 0.045MPa for unreinforced adobe
216 specimens are reported in the literature[22]. It is noted that the test results in the present study are
217 relatively close to what has been reported in the literature. It is evident that fibers endowed the
218 mortar with significant shear strength and friction coefficient. This was attributed to the
219 mechanical interaction between fibers and soil particles that ultimately mobilised resistance to
220 applied shear. The fibers provided large friction surface area with soil particles hence enhanced
221 friction resistance of the fiber composite.

222 *3.3. Prism test*

223 The results of compressive strength and strain of masonry prisms for specimens with
224 unreinforced mortar and bricks (UBUM), specimens with unreinforced bricks and reinforced
225 mortar (UBRM), specimens with reinforced bricks and unreinforced mortar (RBUM) and
226 specimens with reinforced bricks and mortar (RBRM) are shown in Fig. 8. It is shown that
227 compressive strength of reinforced prisms increases linearly to yield strain and reduces to failure
228 strain. The unreinforced prisms fail immediately after reaching yield strain which is an indicative
229 of brittle behaviour. In comparison, prisms with unreinforced mortar mobilise low strength
230 compared with reinforced prisms. It is shown that reinforced prisms exhibit strength increase of a
231 minimum of 25% relative to unreinforced prisms. The ductility increases with fiber inclusion in
232 either the mortar or the bricks. Almost the same compressive strength of about 0.5MPa is
233 mobilised with fiber inclusion in either the mortar or bricks. The prisms with fiber reinforced

234 mortar and bricks show the highest ductility and strength of about 0.55MPa. The yield strain
235 values for UBUM, RBUM, UBRM and RBRM are 0.15%, 0.5%, 1.2% and 1.2%, respectively. It
236 is noted that the strength and deformation of the masonry prisms increase with fiber inclusion
237 especially in the mortar. Nazeen et al [23] reported that strength of the masonry increases with an
238 increase in strength of the mortar. Vicentan and Torrealva [22, 24] in a similar experimental
239 investigation reported values of prism compressive strength of the traditional adobe in the range
240 between 0.36MPa and 1MPa, and strain between 0.5% and 3%. It is noted that the test results are
241 within the values reported in the literature however, the prism compressive strength of adobe
242 masonry depends on the properties of adobe material. The high load carrying capacity of
243 reinforced mortar was responsible for strength improvement of the masonry prisms. The
244 reinforced bricks provided additional strength to the masonry. It can be concluded that the
245 strength of both bricks and mortar had similar influence on the overall strength of the masonry.
246 The typical failure modes of the masonry prisms with unreinforced mortar and bricks (UBUM),
247 with unreinforced bricks and reinforced mortar (UBRM) and those with reinforced bricks and
248 mortar (RBRM) are shown in Fig. 9. It is noted that typical failure mode of unreinforced
249 masonry is characterised by vertical crack across the bricks and mortar joints. Feng Wu [24] also
250 reported similar failure modes of the masonry prisms. In case of the partially reinforced prisms
251 (UBRM), the failure mode is characterised by vertical cracks relatively smaller than those of
252 unreinforced prisms. For the fully reinforced prisms (RBRM), the failure is characterised by both
253 vertical and horizontal cracks accompanied by large lateral deformation. The ductility is
254 advantageous to seismic performance of the reinforced masonry. It implies that the reinforced
255 adobe masonry structure would undergo considerable deformation before collapse during
256 earthquake [25].

3.4. Wallet compression test

257
258 The results of the compressive strength of masonry wallets for reinforced (RBRM) and
259 unreinforced specimens (UBUM) are shown in Table 6. The compressive strength values of the
260 reinforced wallets range between 1.26MPa and 1.33MPa with coefficient of variation of 2.7%.
261 On the other hand, compressive strength of unreinforced wallets ranges between 0.45MPa and
262 0.65MPa with coefficient of variation of 19%. In comparison, the compressive strength values of
263 adobe wallets between 0.77MPa and 1.72MPa are reported in the literature [26]. It is worth
264 noting that compressive strength results from the tests are within the range reported in the
265 literature. It is worth noting that fiber inclusions in the mortar and bricks cause an average
266 increase in the compressive strength of the wallets of about 145% as compared with unreinforced
267 wallets. The results of fiber reinforced masonry wallets show small coefficient of variation
268 (2.7%) while the unreinforced masonry wallets indicate large coefficient of variation (19%). The
269 shrinkage cracks might result in non-uniform material properties and pre-mature failure, and
270 hence were responsible for the scatter of test results for unreinforced wallets. The material
271 homogeneity reduced scatter of the reinforced wallets test results. Failure mode of the reinforced
272 wallets was characterised by large deformation with vertical cracks. On the other hand,
273 unreinforced wallets failed by crushing of the bricks and mortar, as shown in Fig. 10.

3.5. Diagonal compression panel test

274
275 The results of diagonal compression shear strength for reinforced (RBRM) and unreinforced
276 (UBUM) panels are shown in Table 7. The diagonal compression shear strength values of the
277 reinforced panels range between 0.041MPa and 0.056MPa with coefficient of variation of
278 13%. The diagonal shear modulus of reinforced panels ranges between 21.76 and 60.78 MPa. On
279 the other hand, diagonal compression shear strength of unreinforced panels ranges between

280 0.012MPa and 0.016MPa with coefficient of variation of 12.6%. The diagonal shear modulus of
281 unreinforced panels is between 6.48MPa and 13.96MPa. It is noted that reinforced panels exhibit
282 an average increase in shear strength and shear modulus of 235% and 346%, respectively
283 compared with unreinforced panels. The shear stress and strain relationships of both reinforced
284 (RBRM) and unreinforced (UBUM) panels are shown in Fig. 11. It is noted that reinforced
285 panels exhibit considerable ductility before collapse while unreinforced panels show brittle
286 behaviour. The failure modes of both unreinforced and reinforced panel are characterised by the
287 diagonal crack inclined at almost 45° to the horizontal plane of the panel, as shown in Fig. 12a
288 and 12b. The failure modes imply that the major principal tensile stress in this test coincided
289 with the inclination of the crack. It is anticipated that reinforced panel would perform better to
290 lateral loading such as seismic loading.

291 *3.6. Finite element analysis of the wall panels*

292 Finite element modelling was undertaken by imposing loads from the experimental results (81kN
293 and 25kN for reinforced and unreinforced panels, respectively). The major principal tensile stress
294 was assumed to be concentrated at the center of the panel [15, 27, 28]. The modelling scheme of
295 the panel is shown in Fig. 13a and 13b. The results of the finite element linear elastic analysis for
296 unreinforced are shown in Fig. 14a, 14b, 14c and 14d. The results for reinforced panel are shown
297 in Fig. 15a, 15b, 15c and 15d. The finite element results show that the stress and strain are high
298 in the direction inclined at 45° to the horizontal plane of the panel. The normalised principal
299 tensile stresses of about 0.6 and 0.99 for unreinforced and reinforced panels respectively, are
300 indicated. The normalised principal compressive stresses of about 0.96 and 2.7 for unreinforced
301 and reinforced panels respectively, are shown. The corresponding maximum normalised shear
302 stresses of 0.7 and 1.7 for unreinforced and reinforced panels respectively are determined. In the

303 standard interpretation of the masonry diagonal compression test, as provided by ASTM, it is
304 assumed that the stress state at the centre of the panel is of pure shear such that principal tensile
305 stress is equal to shear stress and can be calculated by Eq. 2, and the principal directions coincide
306 with the two diagonals of the panels[15, 21, 28]. According to RILEM, masonry is assumed as an
307 isotropic and homogeneous material such that stress state at the centre of the specimen is not a
308 pure shear state, although the principal directions still coincide with the two diagonals of the
309 panels [15, 16, 28]. This interpretation gives the values of the principal stress state localised at
310 the centre of the panel given by Eq. 4 and Eq. 5.

$$311 \quad \sigma_1 = 0.5 \frac{P_{ult}}{A} \quad (4)$$

$$312 \quad \sigma_3 = 1.62 \frac{P_{ult}}{A} \quad (5)$$

313 where P_{ult} is the ultimate load and A is the net area of the panel.

314 The Mohr circles according to ASTM and RILEM interpretations and the stress state of the
315 simulated reinforced and unreinforced panels are shown in Fig. 16. It can be seen that the
316 numerical analysis results of the reinforced panel agree with RILEM, irrespective of the stress
317 values. The stress state of the unreinforced panel shows slight deviation from the ASTM
318 assumption. It can be concluded that the stress state at the center of the panel for both panels is
319 not a pure shear state and can better be described by RILEM interpretation.

320 **4. Design of vertically and laterally loaded adobe masonry wall**

321 The typical maximum dimensions of adobe houses in the developing countries are
322 8x5x2.5m[29]. The typical thickness is double brick wall of about 250mm.

323 *4.1. Case 1: Vertical Load resistance*

324 The design procedure according to BS5628 [30] and Eurocode 6 [13] is adopted. The design
 325 assumptions and adobe wall specifications include: wall dimensions of 8m length, 2.5m height
 326 and 0.25m thickness, category II of masonry units, normal construction control and material
 327 reduction factor of 3 (Table 2.3 of EC6), simple restraint is provided by the roof, load
 328 eccentricity at the top of the wall is less than $0.005t$ (t is the thickness of the wall), the typical
 329 slenderness ratio is about 10, typical wall capacity reduction factor is 0.97 (Table 7 BS5628).
 330 Vertical load resistance is given by Eq. 6.

$$331 \quad N_r \leq \frac{\beta f_k t}{\gamma_m} \quad (6)$$

332 where $\gamma_m=3$, $\beta=0.97$, f_k is characteristic masonry compressive strength.

333 For unreinforced wall, $f_k=0.5\text{MPa}$ (Refer to results of wallet compressive strength), load
 334 resistance is $N_r \leq 40\text{kN/m}$ run of the wall.

335 For reinforced wall, $f_k=1.3\text{MPa}$, load resistance is $N_r \leq 100\text{kN/m}$ run of the wall.

336 *4.2. Case 2: Lateral shear resistance*

337 Using limit state design approach and maximum vertical load resistance (40N/mm run of
 338 unreinforced wall and 100N/mm run of reinforced wall) and assuming that the wall is fully
 339 vertically loaded, allowable shear resistance of the wall is given by Eq. 7.

$$340 \quad F_r = N_r \tan \phi \quad (7)$$

341 where Φ is the friction angle determined by triplet test, 32° and 39° for unreinforced and
 342 reinforced mortar, respectively.

343 For unreinforced wall, $N_r=40\text{kN/m}$ run of the wall and allowable shear resistance is $F_r \leq 25\text{kN/m}$
 344 run of the wall.

345 For reinforced wall, $N_r=100\text{kN/m}$ run of the wall and allowable shear resistance is $F_r\leq 80\text{kN/m}$
346 run of the wall.

347 **5. Conclusions**

348 The mechanical properties of fiber reinforced and unreinforced adobe masonry were investigated
349 by series of laboratory tests namely, masonry triplet, couplets and prisms tests. The shear
350 strength, tensile bond resistance and compressive strength of the masonry elements were
351 determined. Masonry structural performance was assessed by uniaxial compression and diagonal
352 compression shear tests on wallets and wall panels. Finite element linear elastic analysis was
353 performed to evaluate the stress state condition of both loaded reinforced and unreinforced wall
354 panels. Adobe masonry wall was designed according to BS5628 and Eurocode 6 standards by
355 utilising material properties acquired from the experiments. Based on the acquired results, the
356 following conclusions were drawn;

- 357 1. Fiber inclusion increased tensile resistance of mortar from 28.2N to 37N, representing
358 31% of strength improvement.
- 359 2. Fiber inclusion caused an increase in shear strength of adobe masonry from an average
360 value of 0.028kPa to 0.035kPa with lateral confinement of 0.025kPa. Shear strength
361 increased from 0.085kPa to 0.105kPa with higher lateral confinement of 0.1kPa and fiber
362 inclusion. The corresponding friction coefficient increased from 0.63 to 0.81,
363 representing 22% of improvement.
- 364 3. Fiber inclusion in either the mortar or the bricks caused an increase in the compressive
365 strength of the adobe prisms from 0.4MPa to 0.5MPa, representing 25% of increase. An
366 average strength of wallets increased from 0.53MPa to 1.3MPa with fiber reinforcement
367 in both the mortar and the bricks.

- 368 4. The average shear strength of the adobe wall panels increased from 0.014MPa to
369 0.047MPa while average shear modulus increased from 9.32 MPa to 41.6MPa with fiber
370 inclusion in the mortar.
- 371 5. The shear stress state in the reinforced and unreinforced wall panel was not a pure shear
372 state and was better described by RILEM interpretation.
- 373 6. Fiber reinforced adobe masonry exhibited ductile behaviour and the failure mode of the
374 unreinforced was brittle.
- 375 7. The load resistance of the vertically loaded adobe fiber reinforced masonry wall was
376 estimated as 100kN/m run of the wall while unreinforced wall could support load of
377 approximately 40kN/m run of the wall. The shear resistance of reinforced wall was
378 estimated as 80kN/m run and unreinforced wall could support shear load of about
379 25kN/m run of the wall.

References

- 380 [1] Houben. H and Guillaud. H, Earth Construction: A Comprehensive Guide, IT
381 Publications, London, 1994.
- 382 [2] Walker. P, Bond Characteristics of earth block masonry, J Mater Civ Eng 11(1999) 249-
383 256.
- 384 [3] Mesbah et al, Development of a Direct Tensile Test for Compacted Earth Blocks
385 Reinforced with Natural Fibers, J Mater Civ Eng 16(2004) 95-98.
- 386 [4] Walker. P, Strength and Erosion Characteristics of Earth Blocks and Earth Block
387 Masonry, J Mater Civ Eng 16(2004) 497-506.
- 388 [5] Zami. M S and Le. A, Economic benefits of contemporary earth construction in low-cost
389 urban housing – State-of-the-art review, J Build Appr 5(2010) 259-271.
- 390 [6] Islam. M.S and Iwashita . K, Earthquake resistance of adobe reinforced by low cost
391 traditional materials, J Nat Dis Sci 32(2010) 21.
- 392 [7] Consoli et al, Parameters controlling tensile and compressive strength of fiber-reinforced
393 cemented soil, J Mater Civ Eng (2012).
- 394 [8] Moghal et al, , Effect of polypropylene fibre reinforcement on the consolidation, swell
395 and shrinkage behaviour of lime-blended expansive soil, Int J Geotech Eng 12 (2018)
396 462-471.
- 397 [9] Binici et al, Investigation of fibre reinforced mud brick as a building materia, Constr and
398 Build Mater 19(2005) 313-318.
- 399 [10] Sharma et al, Enhancing sustainability of rural adobe houses of hills by addition of
400 vernacular fiber reinforcement, Inte J of Sustain Built Environ 4(2015) 348–358.
- 401 [11] Blondet et al, Earthquake resistant of earthen construction: The great contemporary
402 experience of Pontifical Catholic University of Peru., Inf Constr 63(2011) 41–50
- 403 [12] Figueiredo et al, Seismic retrofitting solution of an adobe masonry wall, Mater. Struct.
404 46(2013) 203-219.
- 405 [13] ENV 1992-2, Design of masonry structures, CEN, 2006.
- 406 [14] Novelli et al, Seismic Mitigation Framework for Non-engineered Masonry Buildings in
407 Developing Countries: Application to Malawi in the East African Rift, Resilient
408 Structures and Infrastructure, Springer, Singapore, 2019
- 409 [15] Alecci et al, Shear strength of brick masonry walls assembled with different types of
410 mortar, Constr Build Mater 40(2013) 1038–1045.

- 411 [16] RILEM LUMB6, Diagonal tensile strength tests of small wall specimens 1991, Rilem
412 recommendations for the testing and use of constructions materials, RILEM, London,
413 1994, pp. 488–489.
- 414 [17] ASTM C67-03a, Standard test methods for sampling and testing bricks and clay tiles,
415 ASTM, Conshohocken PA, 2003.
- 416 [18] BS EN 1015-11, Methods of test for mortar for masonry. Determination of flexural and
417 compressive strength of hardened mortar, BIS, 1999.
- 418 [19] ASTM C1314-03b, Standard test method for compressive strength of masonry prisms
419 ASTM, Conshohocken PA, 2003.
- 420 [20] BS EN 1052-3, Method of test for masonry: Determination of initial shear strength, BSI,
421 2002.
- 422 [21] ASTM E519-15, Standard test method for diagonal tension (shear), in masonry
423 assemblages, ASTM, Conshohocken PA, 2015.
- 424 [22] Vicente. EF and Torrealva. DE, Mechanical Properties of adobe masonry of historical
425 buildings in Peru, in: F.P.a.M. Chávez, (Ed), 9th Int Conf Structl Anal Histl Constr
426 Mexico City, Mexico 2014.
- 427 [23] Nazeer et al, Behaviour and strength assessment of masonry prisms, Case Stud Constr
428 Mater 8(2018) 23-38.
- 429 [24] Feng Wu , Hong-Nan Li , Jin-Qing Jia, Strength and stress–strain characteristics of
430 traditional adobe block and masonry, Mater Struct 46(2013) 1449–1457.
- 431 [25] Tetley. R and Madabhushi. G, Vulnerability of adobe buildings under earthquake
432 loading, 4th International Conference of Earthquake Geotechnical Engineering Paper No
433 1244, Thessaloniki- Greece, 2007
- 434 [26] Varum et al, Mechanical Characterization of Adobe Masonry Walls in: L.R.a.A.B. Rivera,
435 (Ed), Terra 2008: The 10th International Conference on the Study and Conservation of
436 earthen architectural heritage, Getty Conservation Institute and Mali Ministry of Culture,
437 Bamako Mali, 2008, pp. 307-311
- 438 [27] Gabor et al, Modelling approaches of the in-plane shear behaviour of unreinforced and
439 FRP strengthened masonry panels, Compos Struct 74(2006) 277-288.
- 440 [28] Brignola et al, Identification of shear parameters of masonry panels through the in situ
441 diagonal compression test, Int J Archit Heritage 3(2009) 52–73.
- 442 [29] Novelli et al, A Resource on construction in Earthquake Regions, The World Housing
443 Encyclopedia EERI and IAEE, 2018.
- 444 [30] BS 5628-1, Code of practice for structural use of unreinforced masonry, BSI, London,

445

2005.

Journal Pre-proof

Tables

Table 1 Soil properties used in the study

Soil properties	Value
Specific gravity	2.7
<i>Consistency limits</i>	
Liquid limit (%)	40
Plastic limit (%)	21
Plasticity Index	19
Linear shrinkage (%)	12
USCS	CL
<i>Compaction test</i>	
Maximum dry unit weight (kN/m ³)	17.61
Optimum moisture content (%)	17
<i>Mineral composition (%)</i>	
Al ₂ O ₃	17.05
CaO	8.82
SiO ₂	56.54
Fe ₂ O ₃	7.48
MgO	0.78
K ₂ O	0.35

Table 2 Properties of the sisal fiber used for study.

Fiber property	Value
Breaking tensile strength (MPa)	500
Elongation at break (%)	2.1
Average diameter (mm)	0.2
Young's Modulus (GPa)	23

Table 3 Material properties employed in finite element analysis of panels

Property	Reinforced mortar	Unreinforced mortar	Bricks	Ref
Elastic Modulus (MPa)	150	350	1500	Experiment
Poisson's ratio	0.2	0.2	0.26	

Table 4a Tensile bond resistance of fiber reinforced mud mortar

Specimen Serial	Maximum Tensile capacity (N)	Mean (N)	COV %
RM1	32	37	11
RM2	34		
RM3	40		
RM4	41		
RM5	38		

*RM=Reinforced mortar

Table 4b Tensile bond resistance of unreinforced adobe mud mortar

Specimen Serial	Maximum Tensile capacity (N)	Mean (N)	COV %
URM1	20	28.2	26
URM2	21		
URM3	32		
URM4	37		
URM5	31		

*URM=Unreinforced mortar

Table 5a Shear strength of reinforced mortar with various lateral confinement stresses

Specimen serial	Lateral confinement stress (kPa)		
	0.025	0.05	0.1
Shear strength (MPa)			
1	0.038	0.075	0.105
2	0.035	0.077	0.105
3	0.050	0.075	0.105

Table 5b Shear strength of unreinforced mortar with various lateral confinement stresses

Specimen serial	Lateral confinement stress (kPa)		
	0.025	0.05	0.1
Shear strength (MPa)			
1	0.028	0.035	0.083
2	0.030	0.055	0.085
3	0.038	0.055	0.080

Table 6. Results of compressive strength of fiber reinforced and unreinforced masonry wallets

Specimen designation	Dimensions <i>h x w x t (mm)</i>	Maximum compressive load (kN)	Compressive strength (MPa)	Mean (MPa)	COV %
RMRB1	480 x 400 x 202	126	1.3		
RMRB2	480 x 401 x 205	124	1.26	1.3	2.7
RMRB3	500 x 400 x 209	140	1.33		
UMUB1	502 x 400 x 210	68	0.65		
UMUB2	515 x 410 x 208	48	0.45	0.53	19
UMUB3	520 x 410 x 210	56	0.51		

Table 7 Results of diagonal compression test

Specimen designation	Maximum shear strength (τ) (MPa)	Maximum Diagonal Shear load (kN)	Shear modulus (G) (MPa)	Mean shear strength (MPa)	Mean shear modulus (MPa)	COV shear strength %	COV shear modulus %
UBRM1	0.043	73.6	21.76				
UBRM2	0.041	70.2	42.21	0.047	41.60	13	47
UBRM3	0.056	95.8	60.78				
UBUM1	0.016	27.4	6.48				
UBUM2	0.012	20.5	13.96	0.014	9.32	12.6	44
UBUM3	0.014	24	7.52				

FIGURES

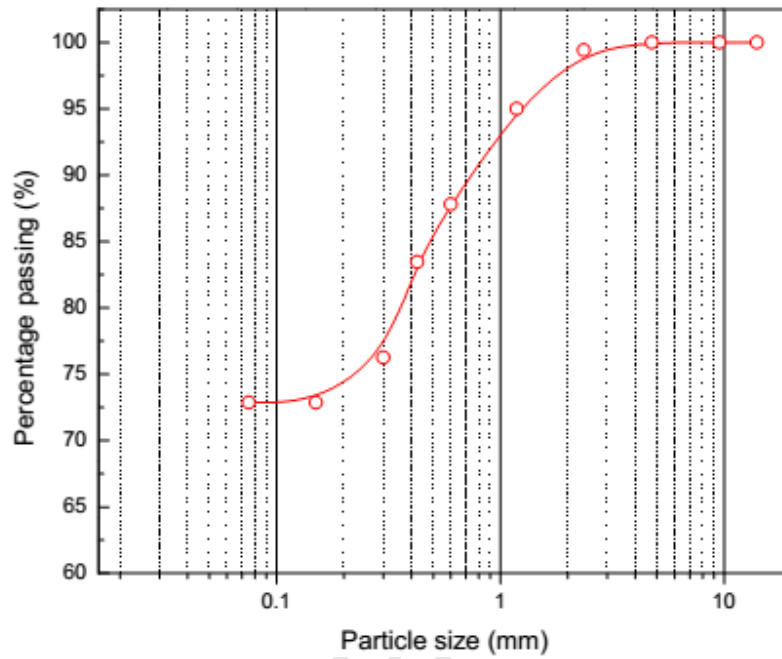


Fig. 1 Grading curve of the soil



Fig. 2 (a) Soil sample (b) mould (c) manufactured adobe bricks (d) sisal fibers used

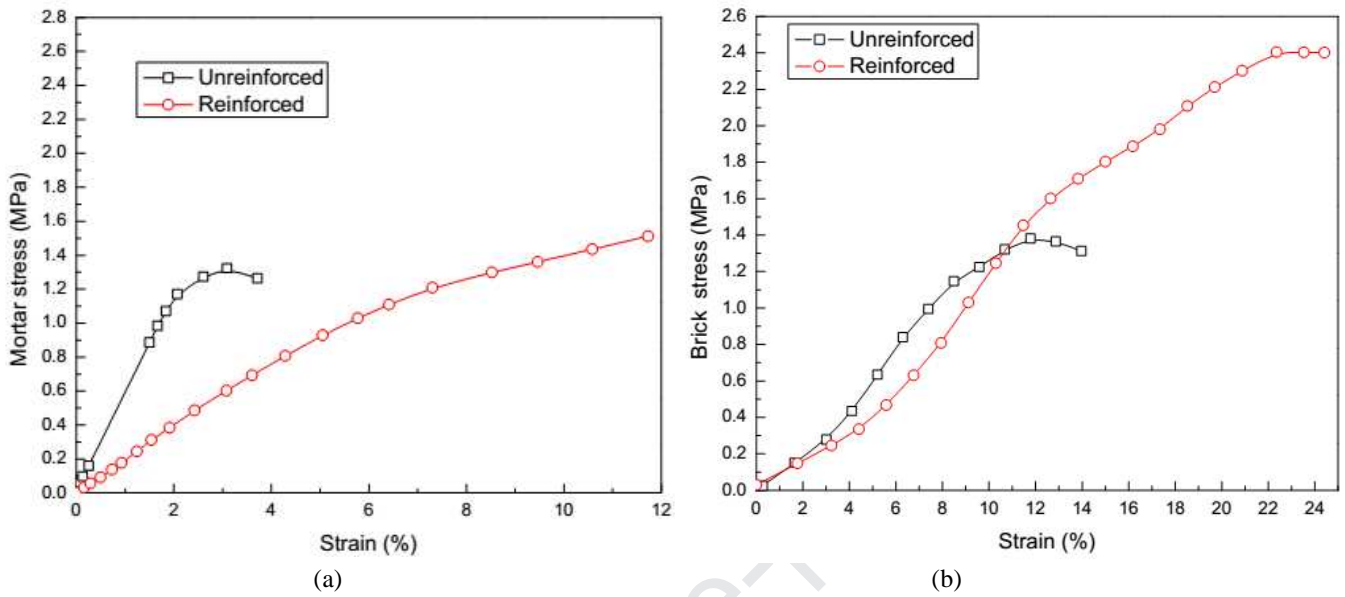


Fig. 3 (a) Typical properties of mortar (b) Typical properties of adobe bricks.



Fig. 4 Test set-up for mortar couplet test

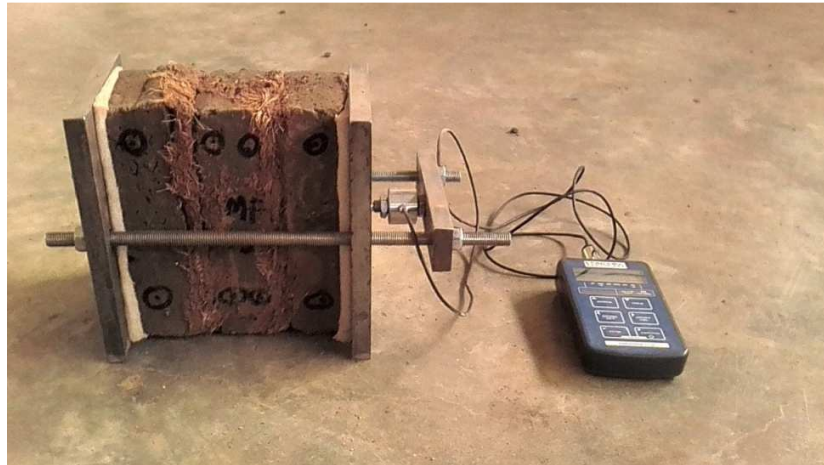


Fig. 5 Triplet test specimen and confinement frame.

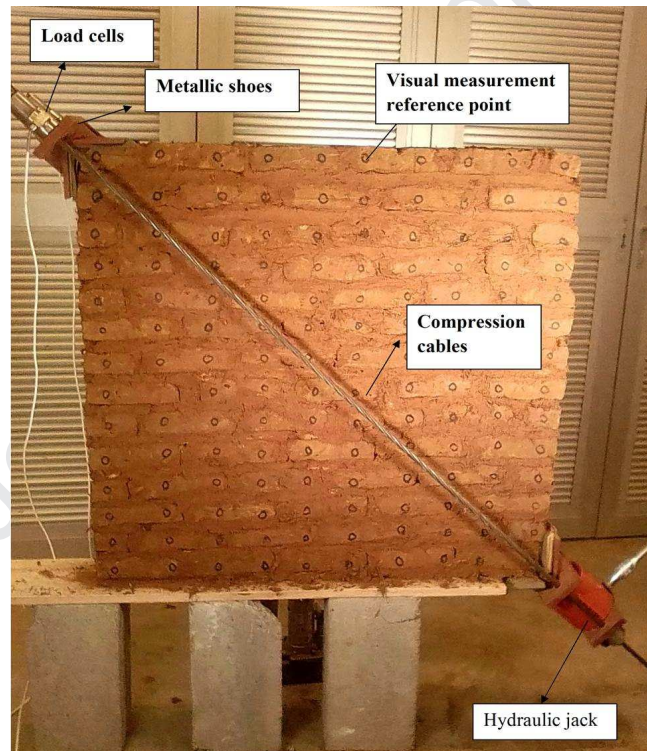


Fig. 6 Diagonal compression test set-up

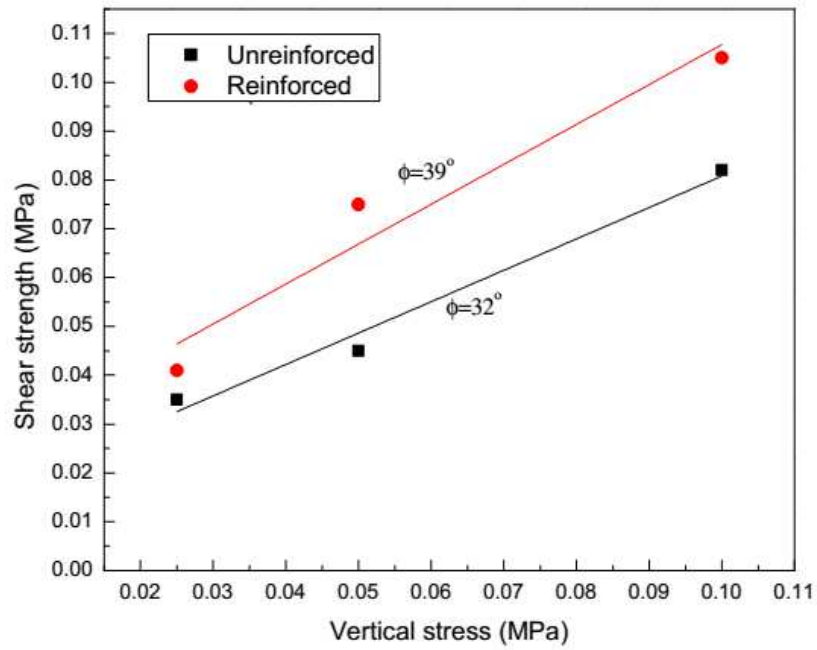


Fig. 7 Mohr-coulomb failure criteria for triplets with reinforced and unreinforced mortar

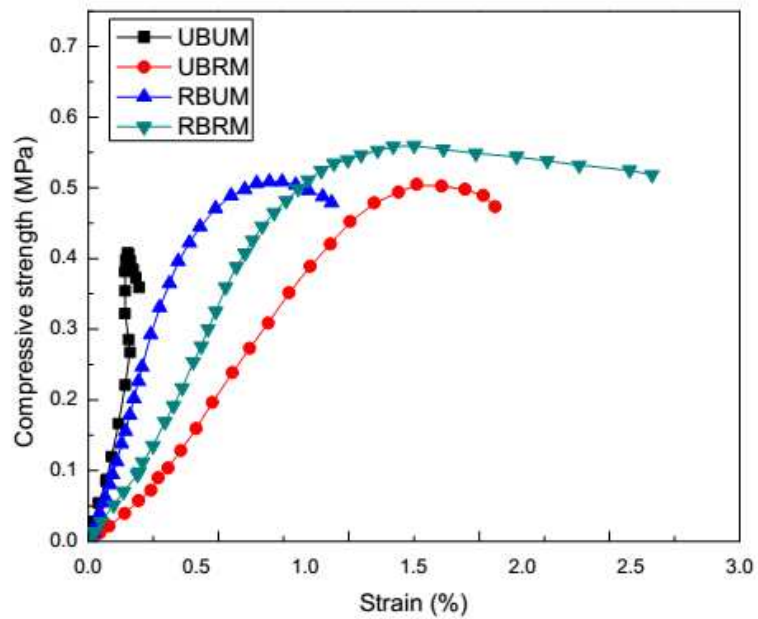


Fig. 8 Stress-strain relationship of masonry prisms

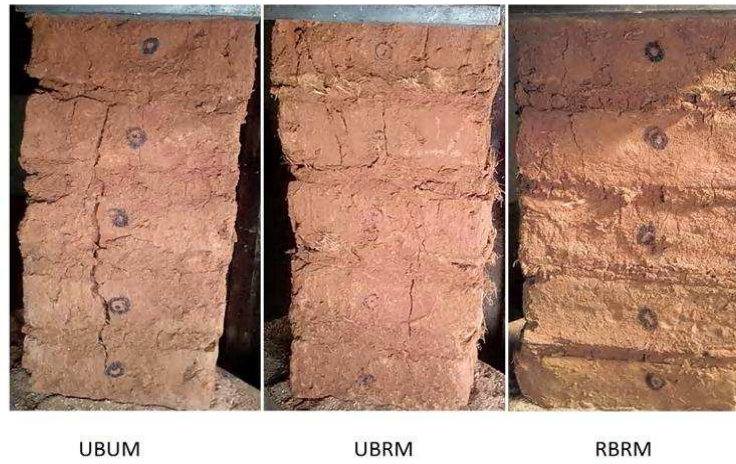


Fig. 9 Failure modes of masonry prisms



(a) (b)
Fig. 10 Failure modes of wallets (a) reinforced (b) unreinforced

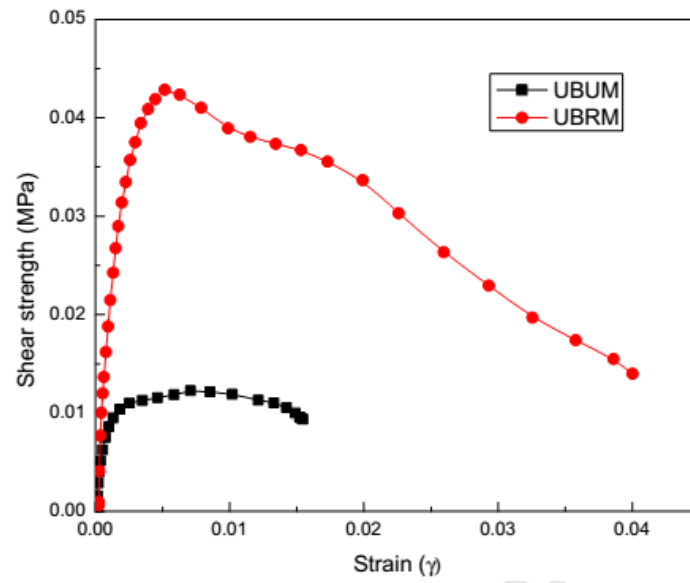
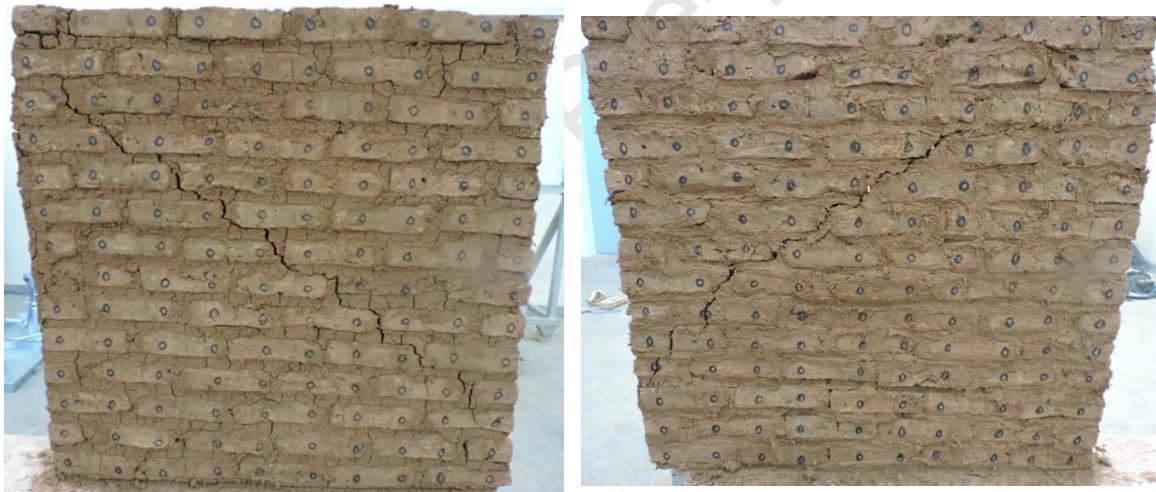


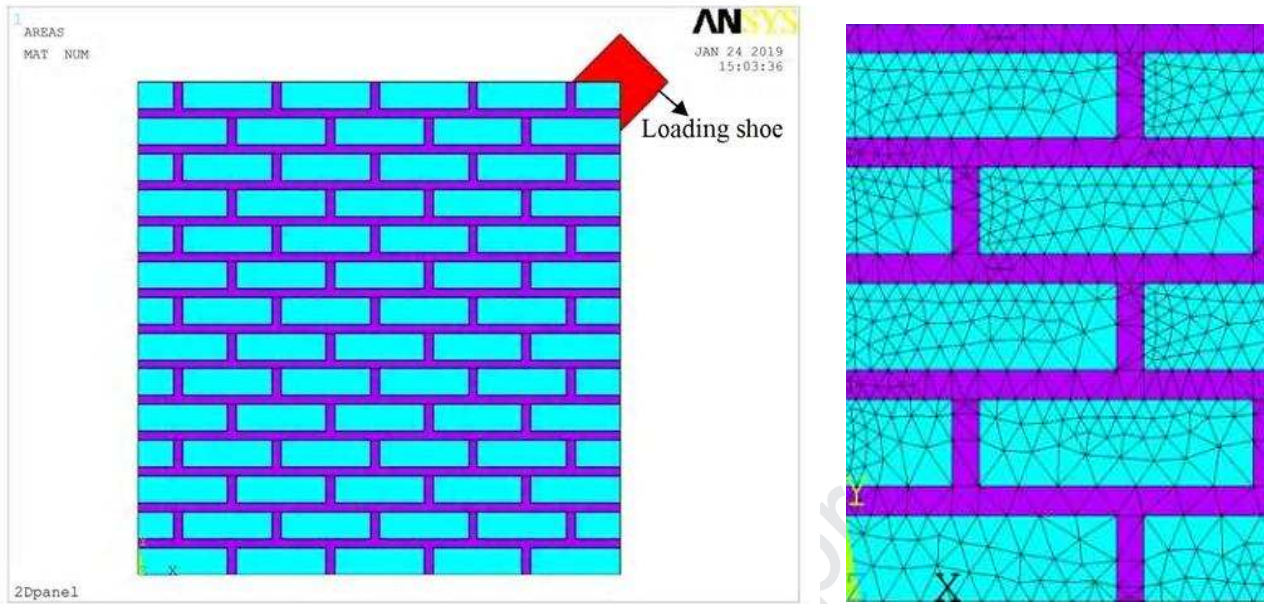
Fig. 11 Shear strength and strain relationship of panels



(a)

(b)

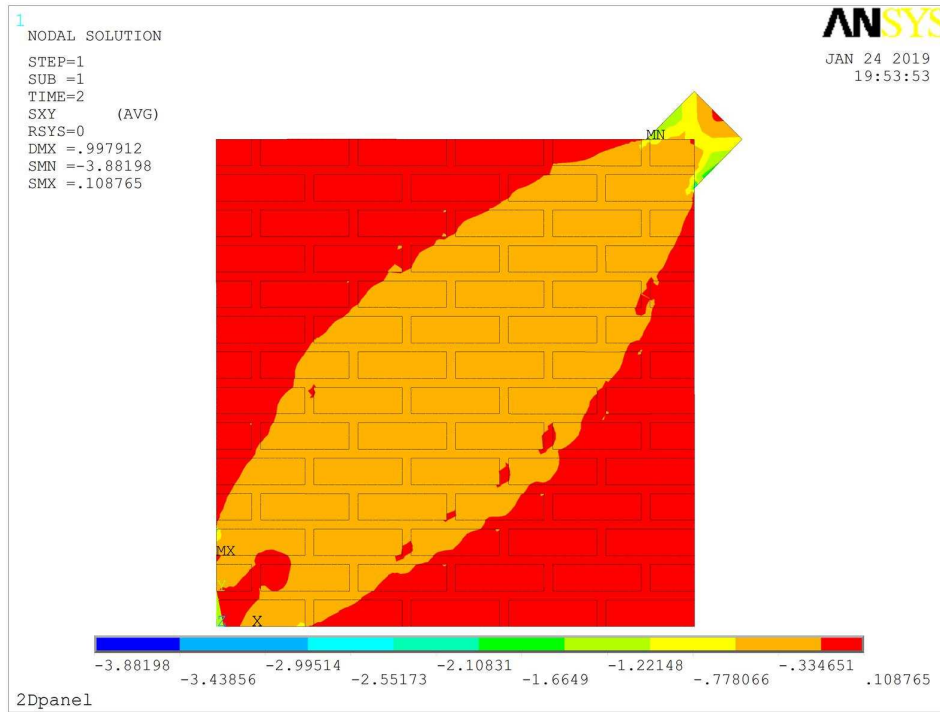
Fig. 12 (a) Failure of unreinforced panel (b) Failure of reinforced mortar.



(a)

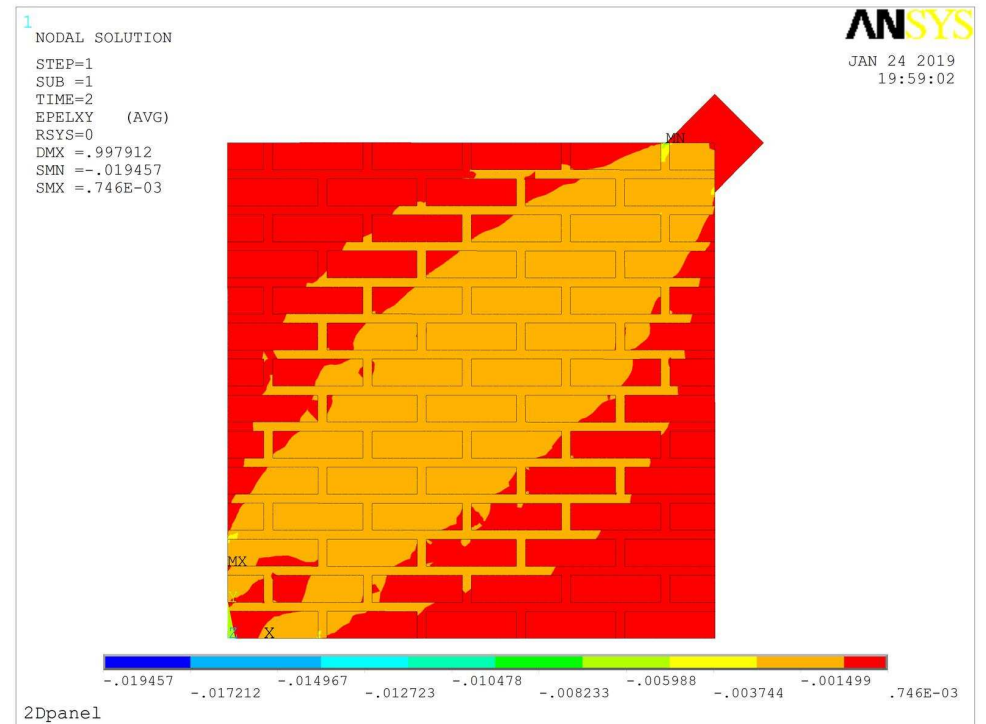
(b)

Fig. 13 (a) Finite Element Analysis Model (b) Triangular element mesh



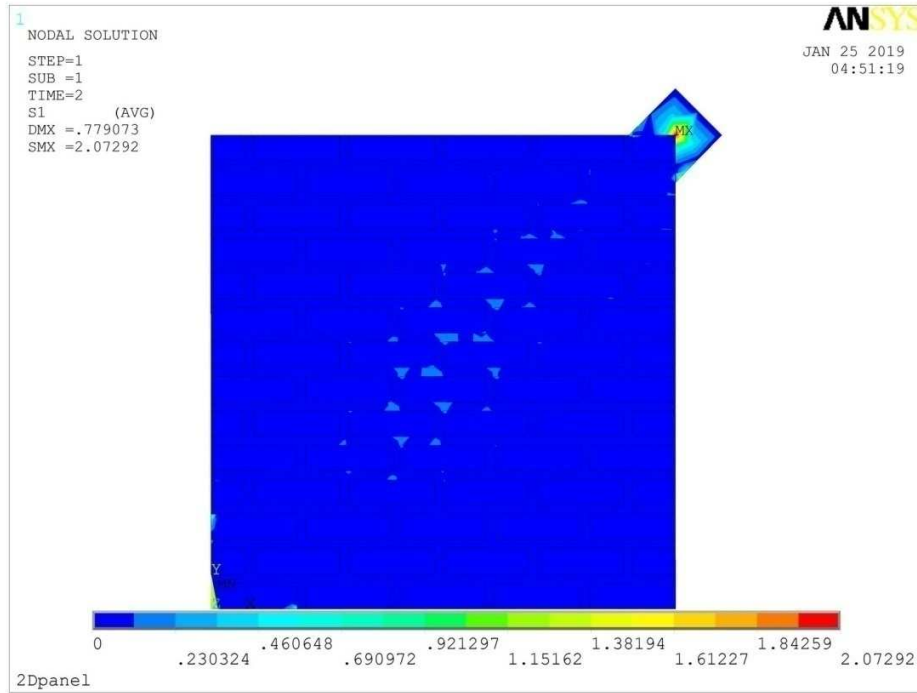
(a)

Fig. 14 (a) Shear stress distribution of unreinforced panel

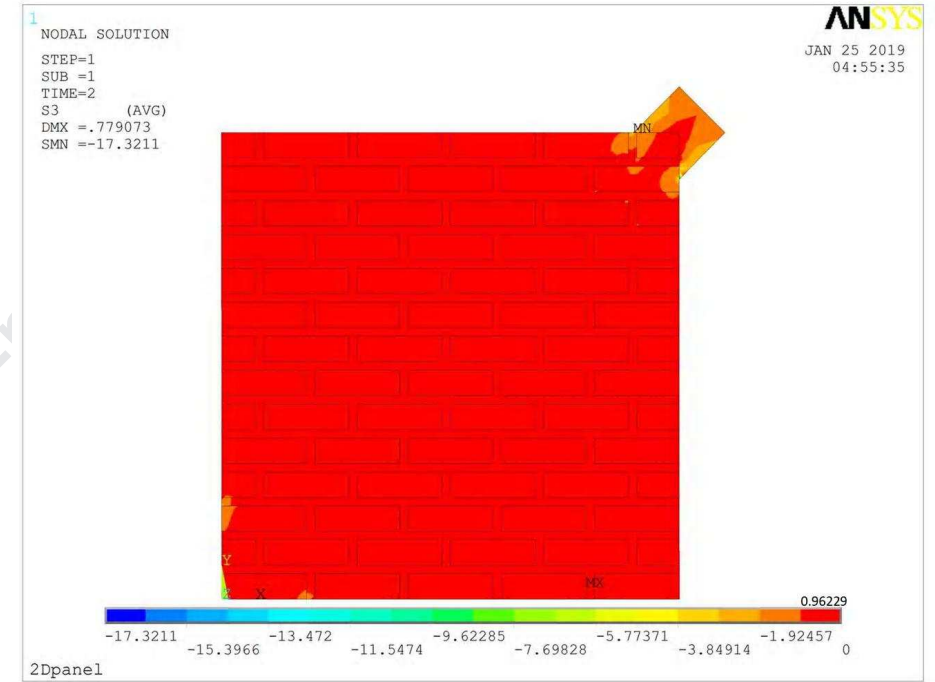


(b)

(b) Shear strain distribution of unreinforced panel



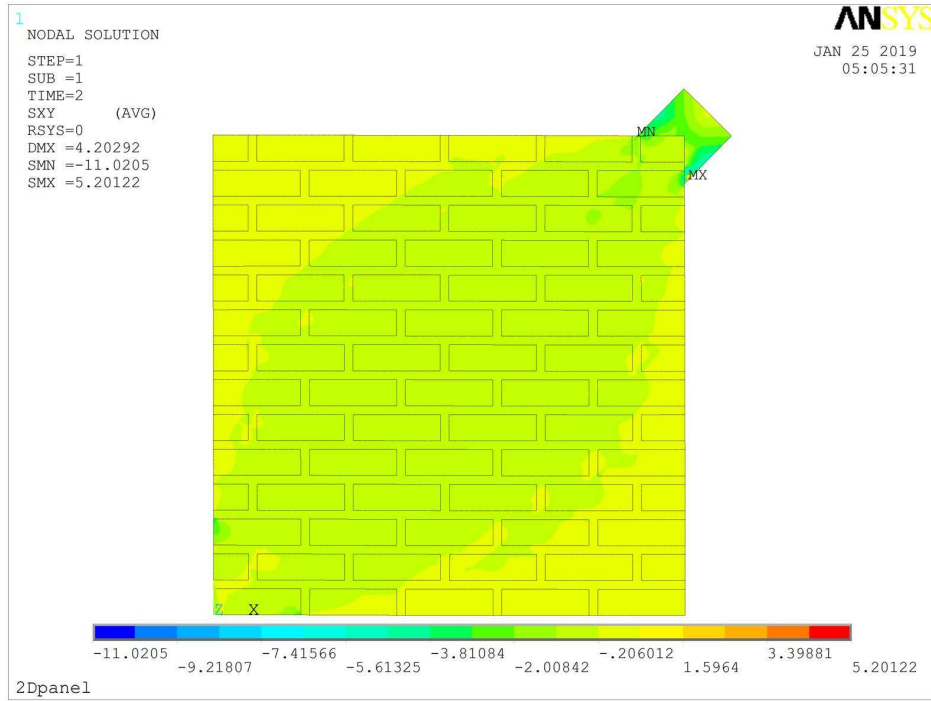
(c)



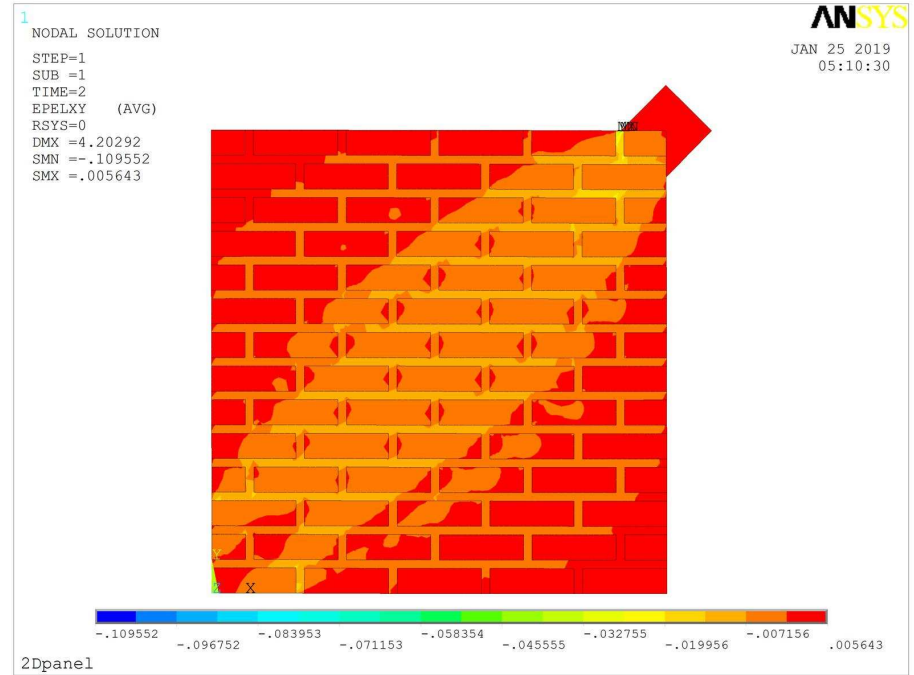
(d)

Fig. 14 (c) Principal tensile stress distribution of unreinforced panel

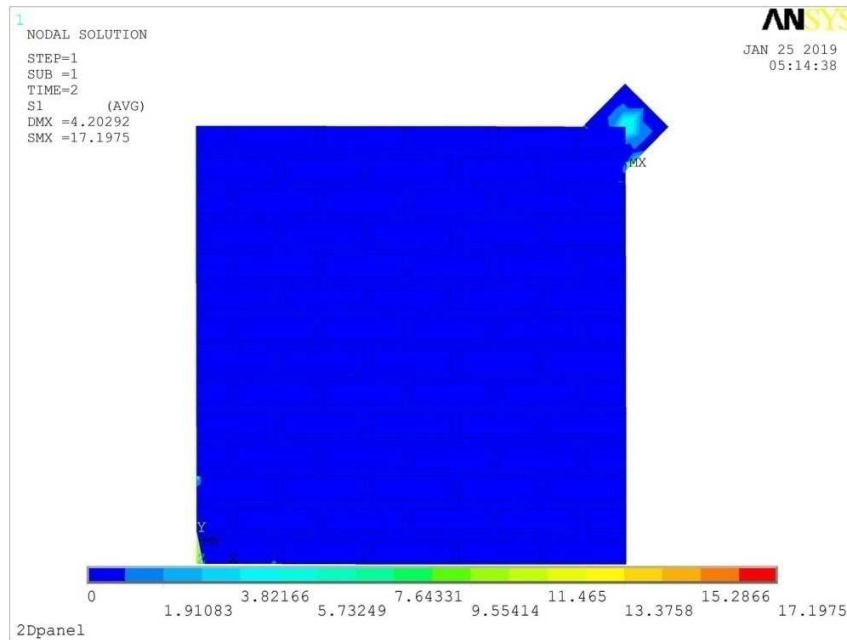
(d) Principal compressive stress distribution of unreinforced panel



(a)
Fig. 15(a) Shear stress distribution of reinforced panel

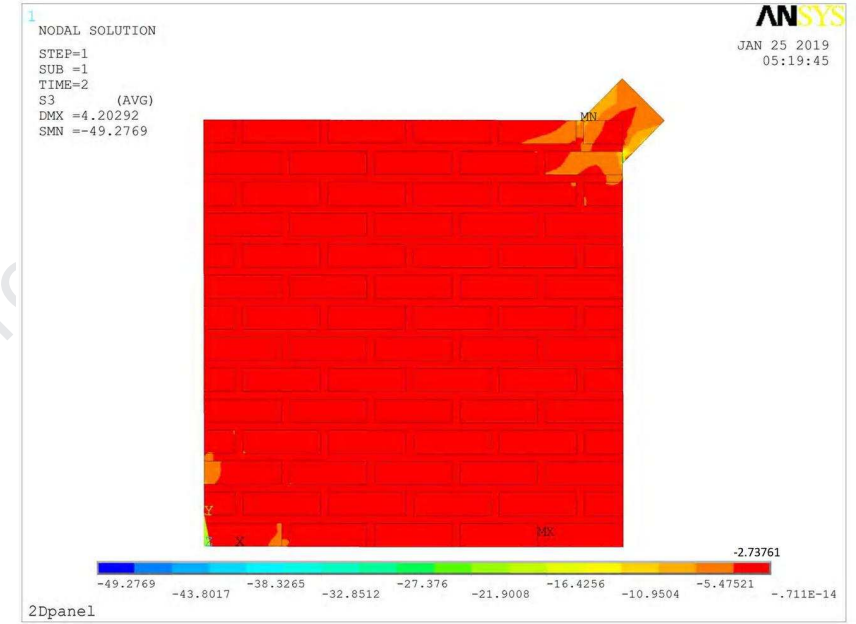


(b)
Fig. 15(b) Shear strain distribution of reinforced panel



(c)

Fig. 15 (c) Principal tensile stress distribution of reinforced panel



(d)

(d) Principal compressive stress distribution of reinforced panel

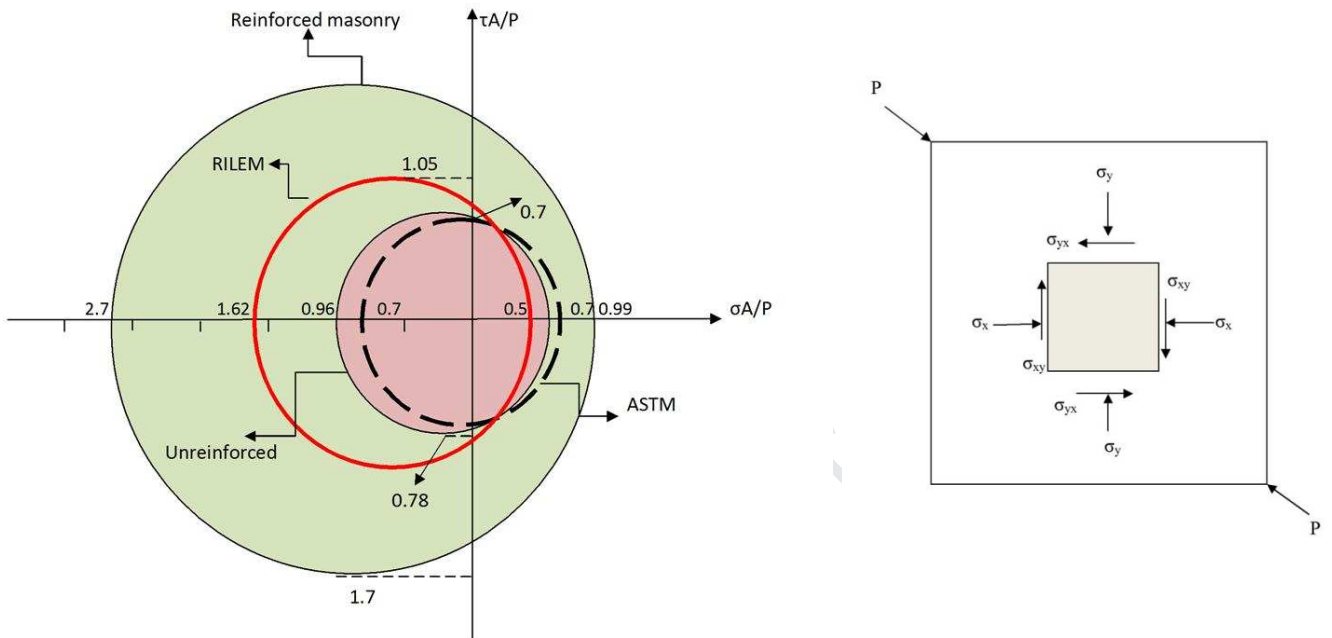


Fig. 16 Normalised Mohr Circles of failure criteria and stress state at the center of the wall panel

Highlights

- Fiber inclusion increases tensile resistance and friction coefficient of adobe masonry.
- The compressive strength of the adobe prisms increases with fiber inclusion in either the mortar or the bricks.
- Shear strength and modulus of adobe masonry panels significantly improve with fiber reinforcement.
- Shear stress state in the reinforced and unreinforced wall panels is not a pure shear state.